

Quenching of Giant Hysteresis Effects in $\text{La}_{1-z}\text{Y}_z\text{H}_x$ Switchable Mirrors

A. T. M. van Gogh, D. G. Nagengast, E. S. Kooij, N. J. Koeman, and R. Griessen

*Faculty of Sciences, Division of Physics and Astronomy, Vrije Universiteit,
De Boelelaan 1081, 1081 HV Amsterdam, The Netherlands*

(Received 2 May 2000)

The giant intrinsic hysteresis as a function of hydrogen concentration x in the optical and electrical properties of the archetypal switchable mirror YH_x is eliminated by alloying Y with the chemically similar La. The $\text{La}_{1-z}\text{Y}_z\text{H}_x$ films with $z \leq 0.67$ are essentially hysteresis-free. The origin of the large hysteresis of alloys with $z \geq 0.86$ is the large uniaxial lattice expansion that accompanies their fcc to hexagonal phase transition in combination with lateral clamping.

PACS numbers: 81.30.-t, 61.50.Ks, 71.30.+h, 78.66.-w

Since the discovery that thin YH_x and LaH_x films show dramatic changes in their optical properties near their metal-insulator (MI) transition when the hydrogen-to-metal ratio x increases from 2 to 3 [1], these materials have attracted a lot of interest because of their technological potential [2–4] and the continuous character of their MI transition, which is still not understood [5–9]. To find experimental clues about what causes YH_3 and LaH_3 to be insulators, the optical, electrical, and structural properties were to be investigated in detail. In this context Kooij *et al.* [10] found that YH_x thin films exhibit anomalously large hysteresis in the optical, electrical, and structural properties as a function of x . During H absorption a two-phase region of face centered cubic (fcc) and hexagonal (hex) structures exists for $1.9 < x < 2.1$ and the MI transition takes place in a *single* hex structural phase [11]. During desorption an fcc-hex two-phase region occurs for $2.0 < x < 2.7$. This desorption behavior is similar to that of bulk YH_x [12], but the absorption behavior is totally different. The term “giant” hysteresis is justified by the difference of 4 orders of magnitude between the ab- and desorption plateau pressures.

In this work we identify the origin of the giant hysteresis by comparing the ab- and desorption behavior of epitaxial and polycrystalline YH_x films and by studying the behavior of thin polycrystalline $\text{La}_{1-z}\text{Y}_z\text{H}_x$ films for various z upon hydrogenation. La is chemically very similar to Y, both having the d^1s^2 valence configuration. This similarity is reflected by the fact that La-Y alloys form a disordered solid solution over almost the whole composition range [13]. However, upon hydrogenation LaH_x behaves completely differently than YH_x . When x changes from 2 to 3 LaH_x stays fcc and contracts [$(\Delta V/V)_{x=2 \rightarrow 3} = -4\%$, with V the volume], whereas YH_x transforms into hex with a large expansion. The chemical similarity and structural difference between La and Y make the $\text{La}_{1-z}\text{Y}_z\text{H}_x$ system particularly suitable to study the role of structural phase transitions on the properties of switchable mirrors.

Thin films are evaporated under UHV conditions ($\sim 10^{-9}$ mbar) by means of molecular beam epitaxy using electron guns. Epitaxial Y films with the c axis perpendicular to the substrate are made on a $\text{CaF}_2(111)$ substrate

as described by Nagengast *et al.* [14]. Polycrystalline $\text{La}_{1-z}\text{Y}_z$ films are made by coevaporation under UHV conditions of the two parent materials on fused quartz substrates (SuprasilTM 1, Heraeus). Evaporation rates are stabilized so as to obtain a composition homogeneity better than 2 at. %. The films are covered with a ~ 10 nm Pd layer that prevents oxidation and catalyses hydrogen absorption. For La-rich films ($z < 0.5$) an AlO_x/Pd composite cap layer is used to avoid Pd diffusion and oxidation [15]. In every evaporation run three identical samples are made: one for x-ray diffraction (XRD)/resistivity measurements, one for optical/resistivity measurements, and one for composition and thickness measurements using Rutherford backscattering and profilometry, respectively.

Optical measurements are done in a Bruker IFS 66/S Fourier-transform infrared spectrometer. The sample is placed in a cell in which a H_2 gas pressure is increased stepwise from 200 to 10^5 Pa. Transmittance spectra are measured alternately ($0.7 < \hbar\omega < 3.5$ eV) and at the same time the resistivity ρ of the film is measured continuously using the van der Pauw method [16]. The desorption of the films is done *in situ*. In principle a film can be desorbed by just pumping away the hydrogen from the cell. However, to increase the desorption kinetics we additionally apply 10^5 Pa of ambient air [17] and heat the sample to a maximum of 150°C . A comparison with electrochemical desorption at room temperature shows that temperature effects on the optical properties and ρ are negligible for our purposes.

In Fig. 1 the hydrogen concentration dependence of the transmittance of a polycrystalline and an epitaxial YH_x film are compared. To determine x we compare ρ during gas loading with its measured value during electrochemical loading [9,18]. During absorption the transmittance first decreases and the lattice structure transforms from fcc to hex. Upon further increase of x , the film opens optically within one single hex structural phase. During hydrogen desorption the fcc-hex two-phase region already starts at $x \approx 2.7$ and ends at $x \approx 2.0$, as in bulk YH_x [12]. For more details on the hysteresis and for a quantitative description of the shape of this curve see Ref. [10]. Important here is that the behavior of *polycrystalline* and *epitaxial*

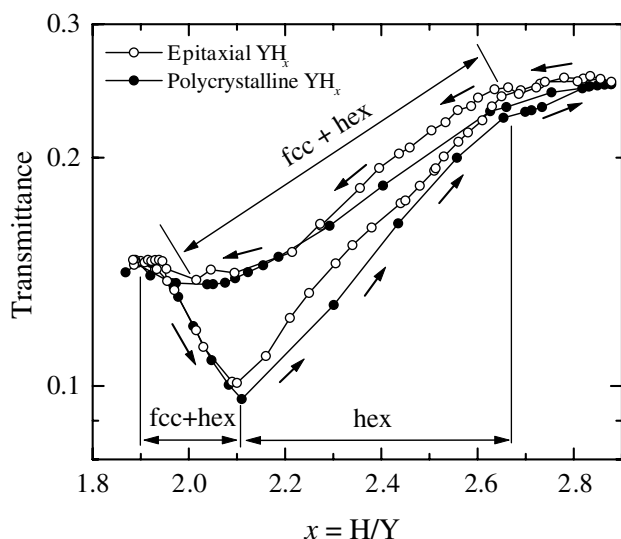


FIG. 1. Hydrogen concentration dependence of the optical transmittance ($\hbar\omega = 1.78$ eV) of a 60 nm epitaxial and a 50 nm polycrystalline Y film. The films are covered with a 10 nm thick Pd cap layer. Both films exhibit a large hysteresis between hydrogen ab- and desorption, reflecting the intrinsic nature of the hysteresis. The thick arrows indicate ab- and desorption path.

YH_x is the same, indicating (i) that the hysteresis is an intrinsic thin film effect and (ii) that a texture with hexagonal planes parallel to the substrate is generated by the first H-absorption in polycrystalline films.

To study the influence of the structural phase transition on the hysteresis, XRD on a series of La-Y alloys is done using a RIGAKU x-ray diffractometer. The sample is mounted in a gas cell with Be windows to enable *in situ* hydrogenation. The scattering angle 2θ is scanned between 20° and 70° and the incident angle θ is kept fixed at 10° . In this way the path length is optimized and many Bragg reflections are measured, optimizing the structural information. Detailed results will be published elsewhere. Important here are (i) the direct observation of the aforementioned texturing of the polycrystalline films during the first hydrogen loading and (ii) the z dependence of the lattice parameters for $x = 2$ and 3 that we will discuss below.

To compare the fcc and hex lattice parameters we define a ($:= a_{\text{hex}}$ and $a_{\text{fcc}}/\sqrt{2}$) and c ($:= c_{\text{hex}}$ and $2a_{\text{fcc}}/\sqrt{3}$). All dihydrides are fcc, with a continuous decrease of a and c as a function of z (see Fig. 2). However, the trihydrides show a transition from fcc to hex between $z = 0.67$ and 0.86 , accompanied by a marked increase of c and a modest decrease of a . Note that for $z > 0.67$ and $x = 3$ the ratio c/a is very large (1.78). This is consistent with the fact that YH_3 does not have the hcp structure, for which in general $c/a < 1.6$ is found [20], but the HoD_3 structure in which the octahedral H atoms have shifted towards the Y hexagonal planes [21,22]. Figure 2 also shows that, as for bulk material, LaH_x contracts when x increases from 2 to 3 [19]. For $z = 0.38 \pm 0.03$ the atomic volume V ($= a^2 c \times \sqrt{3}/4$) is unaffected upon hydrogenation. For $0.38 < z < 0.67$ the material expands.

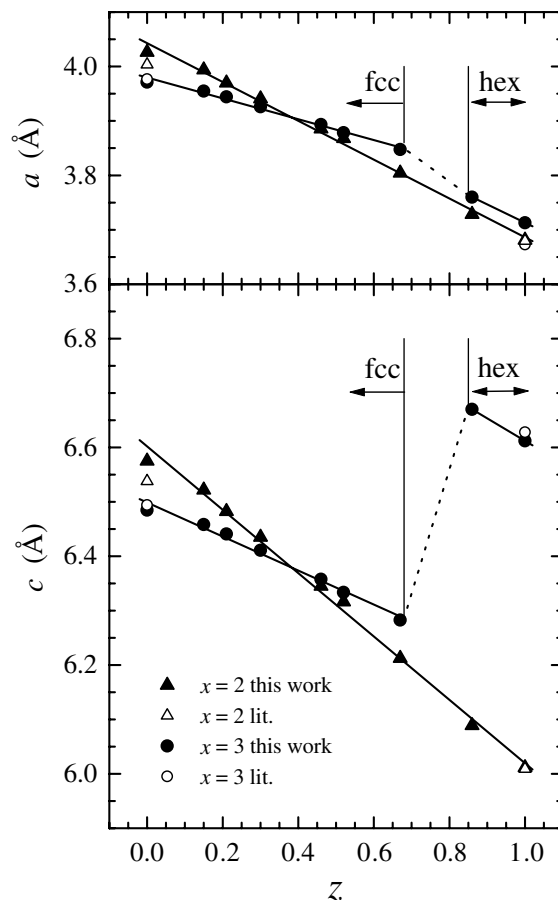


FIG. 2. Lattice parameters of $\text{La}_{1-z}\text{Y}_z\text{H}_x$ as a function of z for the di- and trihydrides. To compare the hex lattice parameters a and c with those of the fcc structure we take $a = a_{\text{fcc}}/\sqrt{2}$ and $c = 2a_{\text{fcc}}/\sqrt{3}$. The errors in the measured values are $\leq 0.1\%$. Literature values for (bulk) YH_x and LaH_x are taken from Ref. [19].

For $z < 0.67$ the value of $|(\Delta V/V)_{x=2 \rightarrow 3}|$ is always smaller than 4%, whereas for the alloys showing the fcc-hex phase transition this value equals $12 \pm 1\%$. As is clear from Fig. 2 the latter value is almost completely determined by the expansion of the c axis: for $z \geq 0.86$ we find $\Delta a/a = 0.85 \pm 0.01\%$ and $\Delta c/c = 9.7 \pm 0.2\%$. In other words, for $z \geq 0.86$ our films expand uniaxially during hydrogenation from the di- to the trihydride (see also Table II of Ref. [10]).

Optical transmittance t versus resistivity is shown in Fig. 3 for seven different alloys. This representation of the experimental data is found to be most suitable for a discussion of hysteretic effects. Their main features are: (i) $\text{La}_{0.14}\text{Y}_{0.86}\text{H}_x$, which also undergoes an fcc-hex transition and exhibits the same behavior upon hydrogen ab- and desorption as YH_x , but with an even larger hysteresis. (ii) The films with $z \leq 0.30$ are completely hysteresis-free and have a very sharp optical transition. (iii) For $0.46 \leq z \leq 0.67$ the optical transition proceeds more gradually with still some hysteresis present. For all films t versus ρ reaches its final shape after the first ab- and desorption cycle, except for the alloy with $z = 0.67$,

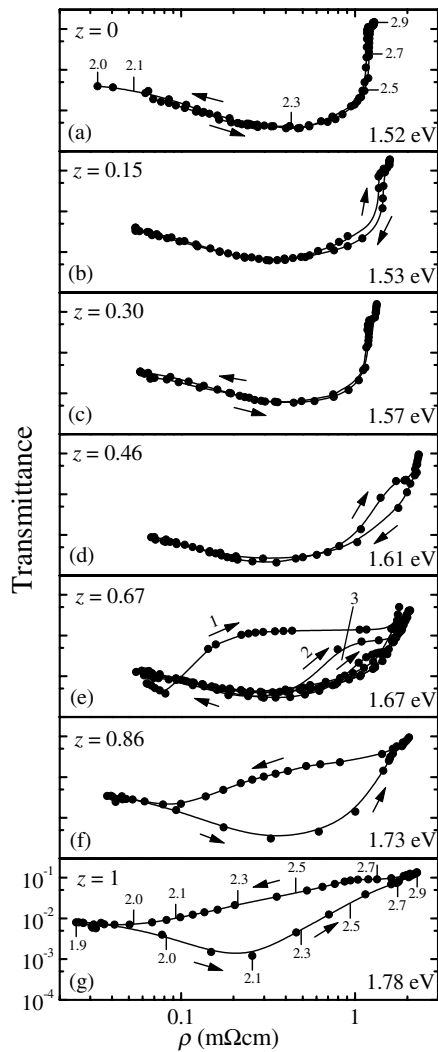


FIG. 3. Optical transmittance as a function of the resistivity ρ during gas phase loading of seven 300 nm thick $\text{La}_{a_{1-z}}\text{Y}_z$ films. The transmittances are given for the photon energy for which the dihydride transmittance has its maximum. The data have not been corrected for the cap layer. For all films the second loading is shown except for $z = 0.67$, for which the first three loading cycles are shown (see labeled arrows). The labels in (a) and (g) indicate hydrogen concentrations as determined electrochemically [18].

which becomes reproducible from the third loading cycle on. This is consistent with the XRD data in Fig. 2, which show that this film is on the borderline of the fcc-hex phase transition.

From the data in Figs. 2 and 3 we conclude that the hysteresis is closely related to the large uniaxial change $\Delta c/c$ between the di- and trihydrides. Note that it is not the magnitude of ΔV (12%) that is important (for example PdH_x exhibits similar volume changes but is only very weakly hysteretic [19,23]), but the fact that ΔV occurs almost entirely uniaxially along the c axis.

We show now that a large uniaxial expansion in combination with lateral clamping can explain the giant hysteresis of Y-rich switchable mirrors. For this let us consider $\text{YH}_{1.9}$ (or an Y-rich alloy with $z \geq 0.86$) with the hexago-

nal planes parallel to the substrate (see Fig. 4). Upon hydrogen absorption from the dihydride [see Fig. 4(a)] a nucleus of hex- $\text{YH}_{2.7}$ is formed, as in a bulk sample, accompanied by a large (9.7%) expansion along the c axis [Fig. 4(b)]. The expansion along the a axis, although modest (0.85%), is important since it ensures a tight lateral mechanical contact with the neighboring fcc- $\text{YH}_{1.9}$, as schematically indicated by springs in Fig. 4. The local c -axis expansion of the hex- $\text{YH}_{2.7}$ nucleus is then able to expand so much the surrounding fcc- $\text{YH}_{1.9}$ nuclei along their c axis that they are mechanically transformed into *hexagonal* $\text{YH}_{1.9}$ [see Fig. 4(c)]. This transformation is easy because enthalpies associated with fcc-hcp transformations are small (~ 1 kJ/mol [24]), since they involve only a change from an $ABCABC\dots$ into an $ABABAB\dots$ stacking of hexagonal planes. Subsequently hydrogen diffuses from the initial hex- $\text{YH}_{2.7}$ nucleus to the neighboring hex- $\text{YH}_{1.9}$ until diffusive equilibrium is reached [see Fig. 4(d)], resulting in a fully hexagonal film with an overall hydrogen concentration $x = 2.1$ and a high lateral stress state [indicated by the compressed springs in Fig. 4(d)]. Further hydrogenation from $x = 2.1$ to 2.9 happens within the hexagonal structural phase and without additional strains [see Figs. 1 and 3(a) and Ref. [10]].

Since lateral clamping plays an essential role in the proposed scenario it is evident that the hydrogen *desorption* behavior is totally different. The asymmetry with the absorption case lies in the stress state. When during desorption the first fcc- $\text{YH}_{2.0}$ nucleus is formed within the hex- $\text{YH}_{2.7}$ matrix it shrinks and instead of transforming the surrounding hex- $\text{YH}_{2.7}$ into fcc, stress is relieved, resulting in a broad two-phase region consisting of fcc- $\text{YH}_{2.0}$ and hex- $\text{YH}_{2.7}$, as in bulk. This leads to the observed large hysteresis effects.

Within this interpretation the deviating behavior of the $\text{La}_{0.33}\text{Y}_{0.67}\text{H}_x$ film (Fig. 3) during the first three loading cycles is naturally understood as annealing by a reordering of crystallites upon subsequent hydrogen ab- and desorption cycles.

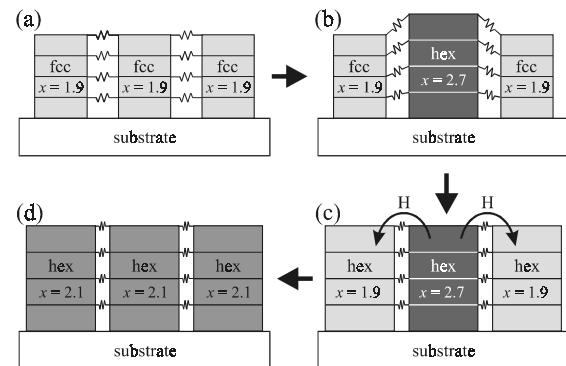


FIG. 4. Schematic drawing of the lateral clamping mechanism, proposed to explain the origin of the large hysteretic effects in $\text{La}_{1-z}\text{Y}_z\text{H}_x$ for $z > 0.67$. The horizontal lines in the depicted crystallites denote hexagonal lattice planes ($\{111\}$ in fcc and $\{001\}$ in hex).

The proposed scenario can also explain a curious effect observed by den Broeder *et al.* in a lateral hydrogen diffusion experiment in an yttrium film [25]. They observed that the front corresponding to the $\alpha^* - \beta$ phase transition, which is accompanied by a small 5% volume increase, was completely smooth while the $\beta - \gamma$ front, accompanied by the large 12% volume increase, was rough [26]. Furthermore, the $\alpha^* - \beta$ front moved smoothly, while the $\beta - \gamma$ front developed bursts in which micron-sized regions of β -YH_x (fcc) suddenly transformed into γ -YH_x (hex). These bursts are the fingerprints of the strain induced transformation of fcc-YH_{2+ δ} into hex-YH_{2+ δ} .

The existence of mechanical interactions on a micrometer length scale is also consistent with the recent observation of *domain switching* observed by Kerssemakers *et al.* in epitaxial YH_x films [27]. In these films, which exhibit excellent crystallinity, there is a regular triangular network with a size of the order of 1 μ m. Within such a domain β -YH_x switches as a whole to γ -YH_x, the ridges accommodating the lattice deformation.

In conclusion, the giant hysteresis in Y-rich switchable mirror films is caused by a combination of the large uniaxial lattice expansion that accompanies the fcc-hex phase transition and lateral clamping. La-rich films, for which $(\Delta V/V)_{x=2 \rightarrow 3} < 0$, are completely hysteresis-free and have a very sharp optical transition. This sharp transition is very attractive for a study of the continuous MI transition in these systems. It is also relevant for technological applications, as the power necessary to switch an optical device is linearly proportional to the amount Δx of hydrogen involved in the switching.

We wish to thank S.J. van der Molen and J.W.J. Kerssemakers for fruitful discussions. This work is part of the research program of the Stichting voor Fundamenteel Onderzoek der Materie (FOM), financially supported by the Nederlandse Organisatie voor Wetenschappelijk Onderzoek (NWO) and Philips Research, and of the TMR Research Network "Metal-hydride films with switchable physical properties."

[1] J. N. Huiberts, R. Griessen, J. H. Rector, R. J. Wijngaarden, J. P. Dekker, D. G. de Groot, and N. J. Koeman, *Nature* (London) **380**, 231 (1996).
 [2] P. van der Sluis, M. Ouwkerk, and P. A. Duine, *Appl. Phys. Lett.* **70**, 3356 (1997).
 [3] R. Armitage, M. Rubin, T. Richardson, N. O'Brien, and Yong Chen, *Appl. Phys. Lett.* **75**, 1863 (1999).
 [4] R. Griessen and P. van der Sluis, *Phys. Unserer Zeit* (to be published).

[5] J. N. Huiberts, R. Griessen, R. J. Wijngaarden, M. Kremers, and C. Van Haesendonck, *Phys. Rev. Lett.* **79**, 3724 (1997).
 [6] P. J. Kelly, J. P. Dekker, and R. Stumpf, *Phys. Rev. Lett.* **78**, 1315 (1997).
 [7] K. K. Ng, F. C. Zhang, V. I. Anisimov, and T. M. Rice, *Phys. Rev. Lett.* **78**, 1311 (1997); *Phys. Rev. B* **59**, 5398 (1999).
 [8] R. Eder, H. F. Pen, and G. A. Sawatzky, *Phys. Rev. B* **56**, 10 115 (1997).
 [9] A. T. M. van Gogh, E. S. Kooij, and R. Griessen, *Phys. Rev. Lett.* **83**, 4614 (1999).
 [10] E. S. Kooij, A. T. M. van Gogh, D. G. Nagengast, N. J. Koeman, and R. Griessen, *Phys. Rev. B* (to be published).
 [11] YH₃ does not have the hcp structure but the slightly different HoD₃ structure [21,22].
 [12] L. N. Yannopoulos, R. K. Edwards, and P. G. Wahlbeck, *J. Phys. Chem.* **69**, 2510 (1965).
 [13] K. A. Gschneidner, Jr. and F. W. Calderwood, *Bull. Alloy Phase Diagrams* **3**, 94 (1982).
 [14] D. G. Nagengast, J. W. J. Kerssemakers, A. T. M. van Gogh, B. Dam, and R. Griessen, *Appl. Phys. Lett.* **75**, 1724 (1999).
 [15] A. T. M. van Gogh, S. J. van der Molen, J. W. J. Kerssemakers, N. J. Koeman, and R. Griessen, *Appl. Phys. Lett.* **77**, 815 (2000).
 [16] L. J. van der Pauw, *Philips Res. Rep.* **13**, 1 (1958).
 [17] L. Grasjo, G. Hultquist, K. L. Tan, and M. Seo, *Appl. Surf. Sci.* **89**, 21 (1995).
 [18] E. S. Kooij, A. T. M. van Gogh, and R. Griessen, *J. Electrochem. Soc.* **146**, 2990 (1999).
 [19] W. M. Mueller, J. P. Blackledge, and G. G. Libowitz, *Metal Hydrides* (Academic Press, New York, 1968).
 [20] K. N. R. Taylor and M. I. Darby, *Physics of Rare Earth Solids* (Chapman and Hall, London, 1972).
 [21] A. Remhof, G. Song, Ch. Sutter, A. Schreyer, R. Siebrecht, H. Zabel, F. Güthoff, and J. Windgasse, *Phys. Rev. B* **59**, 6689 (1999).
 [22] T. J. Udovic, Q. Huang, and J. J. Rush, *J. Phys. Chem. Solids* **57**, 423 (1996).
 [23] M.-W. Lee and R. Glosser, *J. Appl. Phys.* **57**, 5236 (1985).
 [24] *CRC Handbook of Chemistry and Physics* (CRC Press, Boca Raton, 1996–1997), 77th ed., pp. 4–115.
 [25] F. J. A. den Broeder, S. J. van der Molen, M. Kremers, J. N. Huiberts, D. G. Nagengast, A. T. M. van Gogh, W. H. Huisman, J. P. Dekker, N. J. Koeman, B. Dam, J. H. Rector, S. Plota, M. Haaksma, R. M. N. Hanzen, R. M. Jungblut, P. A. Duine, and R. Griessen, *Nature* (London) **394**, 656 (1998).
 [26] The α^* , β , and γ phase correspond to the dilute hcp YH_{x<0.25} phase, the dihydride and the trihydride phase, respectively. Note that the γ -YH_x phase exists already for $x > 2.1$ during H-absorption.
 [27] J. W. J. Kerssemakers, S. J. van der Molen, N. J. Koeman, R. Günther, and R. Griessen, *Nature* (London) **406**, 489 (2000).